Atmos. Chem. Phys. Discuss., 2, 875–903, 2002
www.atmos-chem-phys.org/acpd/2/875/

Atmospheric Chemistry and Physics Discussions

Redistribution of trace gases by convective clouds – mixed-phase processes

Y. Yin, K. S. Carslaw, and D. J. Parker

Institute for Atmospheric Science, School of the Environment, University of Leeds, Leeds, UK

Received: 10 May 2002 – Accepted: 12 June 2002 – Published: 24 June 2002

Correspondence to: Y. Yin (yan@env.leeds.ac.uk)

Abstract

The efficiency of gas transport to the free and upper troposphere in convective clouds is investigated in an axisymmetric dynamic cloud model with detailed microphysics. In particular, we examine the sensitivity of gas transport to the treatment of gas uptake by different ice hydrometeors. Two parameters are used to describe this uptake. The gas retention coefficient defines the fraction of dissolved gas that is retained in an ice particle upon freezing, which includes also the riming process. We also define a gas burial efficiency defining the amount of gas entrapped in ice crystals growing by vapour diffusion. Model calculations are performed for continental and maritime clouds using a complete range of gas solubilities, retention coefficients and burial efficiencies. The results show that the magnitude of the gas retention coefficient is much more important for gas transport in maritime clouds than in continental clouds. The cause of this difference lies in the different microphysical processes dominating the formation and evolution of hydrometeors in the two cloud types. For highly soluble gases, the amount of gas transported to the free troposphere in maritime clouds falls approximately linearly by a factor of 12 as the retention coefficient is varied between 0 and 1. Gas transport is relatively insensitive to the magnitude of the gas burial efficiency. However, the burial efficiency strongly controls the concentration of trace gases inside anvil ice crystals, which subsequently form cirrus clouds.

1. Introduction

Convective cloud transport is a primary mechanism for moving trace gas species from the boundary layer to the free troposphere or even lower stratosphere (e.g. Chatfield and Crutzen, 1984; Dickerson et al., 1987; Prather and Jacob, 1997; Barth et al., 2001; Yin et al., 2001). In our previous paper (Yin et al., 2001) we developed a spectral treatment of gas scavenging within a two-dimensional cloud model to investigate trace gas vertical redistribution in precipitating continental and maritime clouds without ice

ACPD

2, 875–903, 2002

formation. The simulations revealed a clear pattern of behaviour depending on gas solubility. The transport of low solubility gases (with effective Henry's law constants $H^* < 10^3$ mol dm^{-3} atm^{-1}) was found to be essentially identical to that of an insoluble tracer. All highly soluble gases ($H^* > 10^6$ mol dm^{-3} atm^{-1}) were also found to behave in a nearly identical way to each other, independent of their solubility. On the other hand, the transport of moderately soluble gases (H^* between 10^3 and 10^6 mol dm^{-3} atm^{-1}) depends on the precise value of H^*.

In this study we extend the treatment of gas scavenging to include ice-phase particles with special attention being paid to the mass transfer between different hydrometeor types induced by drop-ice interactions. Besides dissolution of the gas into liquid drops, scavenging of a gas in ice- or mixed-phase clouds involves two additional processes: the direct uptake of the gas by ice particles and gas mass transfer between the aqueous phase and ice phase due to freezing and riming.

Extensive laboratory and field studies have been conducted by others to investigate the uptake by ice particles of some chemical species found in clouds, including SO_2, HCl, HNO_3, HBr, H_2O_2 (e.g. Sommerfeld and Lamb, 1986; Clapsaddle and Lamb, 1989; Valdez et al., 1989; Mitra et al., 1990; Conklin et al., 1993; Conklin and Bales, 1993; Diehl et al., 1995; Santachiara et al., 1995; Zondlo et al., 1997; Diehl et al., 1998; Hudson et al., 2001; Clegg and Abbatt, 2001). These studies show that the gas uptake depends on many factors, including partial pressure, temperature, surface acidity, and even whether the ice phase is growing or not (e.g. Diehl et al., 1995; Clegg and Abbatt, 2001). However, due to the lack of a theoretical framework to properly describe the contributions from these factors, it is difficult to include this process into cloud chemistry models. In an idealized simulation using a global chemical transport model, Crutzen and Lawrence (2000) investigated the sensitivity of trace gas removal by the ice particles by introducing ice-phase Henry's Law constants $H_{i,x}$ ('i' stands for 'ice'), which were assumed to be proportional to the gas-liquid solubility ($H_{i,x} = r_i H^*_x$, where $r_i \leq 1$), and found that inclusion of ice uptake essentially extended the vertical region of gas scavenging.

ACPD
2, 875–903, 2002

During formation and growth of ice phase hydrometeors via freezing or riming, trace chemical species originally in the aqueous phase may be excluded or retained in the growing ice phase particles. The retention coefficient (R_c in this study), which is the ratio of the concentration of solute retained in the ice phase to that in the parent liquid phase, has been measured by many investigators (e.g. Lamb et al., 1987; Iribarne et al., 1990; Snider et al., 1992; Santachiara et al., 1995). R_c values range from 0.01 to unity, depending on the trace species, but sometimes different R_c values were also reported for the same tracer. For example, Lamb et al. (1987) observed that the entrapped fraction of SO_2 was strongly temperature dependent and ranged from about 0.01 near 0°C to more than 0.12 at −20°C. On the other hand, Iribarne et al. (1990) reported an average value R_c = 0.62 independent of temperature and SO_2 concentration. In another experiment for highly soluble gases such as HCl, HNO_3, H_2O_2, Iribarne and Pyshnov (1990) measured R_c of about unity, but a value of only 0.3 was observed for H_2O_2 by Snider et al. (1992) in natural clouds.

Mari et al. (2000) examined the transport and scavenging of several gas species, including CO, CH_3OOH, CH_2O, H_2O_2, HNO_3, and SO_2, in tropical deep convection, using a one-dimensional entraining/detraining plume model. They noticed that while both HNO_3 and H_2O_2 were efficiently scavenged in the lower (warm) part of the cloud, H_2O_2 was released as the cloud froze due to the low retention efficiency during riming.

In a numerical simulation of the fate of soluble gases in mid-latitude convection, Barth et al. (2001) considered two extreme cases for the interaction of the gas with cloud hydrometeors. The first case assumed that the dissolved gas in the cloud water or rain completely degassed when the parent hydrometeor was converted to ice-phase hydrometeors. The second case assumed that the dissolved tracer was retained in the ice-phase particles. They found that when soluble tracers were degassed, both low and high solubility tracers were transported to the upper troposphere. When tracers were retained in ice hydrometeors, the highly soluble tracers were not ultimately transported to the upper troposphere, but instead were precipitated out of the upper troposphere by snow and hail.

ACPD
2, 875–903, 2002

In this study, numerical simulations are performed to understand how gas transport in mixed-phase precipitating clouds is influenced by hydrometeor transformations and uptake of gases by ice-phase particles. For this purpose, the spectral treatment of gas scavenging in Yin et al. (2001) has been extended to include ice-phase hydrometeors and incorporated into an axisymmetric non-hydrostatic cloud model with detailed microphysics. As in our previous study, we do not restrict our simulations to specific gases under specific conditions. Rather, we examine both continental and maritime clouds and use a complete range of gas solubilities, retention coefficients and uptake efficiencies on to ice particles. We take this approach in order to understand the overall importance of the ice phase in gas transport and, in particular, the implications of gas-ice interaction parameters being poorly constrained by experiments and theory.

A brief description of the model is given in Sect. 2, followed by the initial conditions for the simulations and design of the numerical experiments in Sect. 3. In Sect. 4, the main results are presented, and discussions and summaries are given in Sect. 5.

2. Model description

2.1. The model dynamics and microphysics

The dynamic framework and microphysical processes of an axisymmetric nonhydrostatic anelastic convective cloud model developed by Reisin et al. (1996) were used in this study and will be only briefly described here. The improved calculation of some of the microphysical processes such as drop nucleation, immersion freezing of drops, presented by Yin et al. (2000), were also introduced. In the model, a set of dynamic equations were solved for the vertical and radial velocity, the pressure perturbation, the virtual potential temperature perturbation, the specific humidity perturbation, the specific concentration of aerosols, the specific number and mass for each type of cloud particles in a spectral bin, and concentration of activated ice nuclei.

The warm microphysical processes included are: nucleation of drops, condensation

ACPD
2, 875–903, 2002

and evaporation, collision–coalescence, and binary breakup (Low and List kernel). The ice microphysical processes included are: ice nucleation (deposition, condensation-freezing, contact nucleation, and immersion freezing), ice multiplication, deposition and sublimation of ice, ice–ice and ice–drop interactions, melting of ice particles, and sedimentation of drops and ice particles. All these microphysical processes are formulated and solved using the method of Multi-Moments (Tzivion et al., 1987; Reisin et al., 1996). Four species of hydrometeor are considered: drops, ice crystals, graupel particles and aggregates (snowflakes). The density of the graupel is assumed to be 0.4 g cm^{-3}, while the ice crystal density varies from 0.9 g cm^{-3} for the smallest particles, down to 0.45 g cm^{-3} for the biggest. The density for the aggregates is fixed at 0.2 g cm^{-3}. Each particle species is divided into 34 bins with mass doubling for adjacent bins ($m_{k+1} = 2m_k, k = 1, \cdots 34$). The masses at the beginning of the first bin and the end of last bin for both liquid and solid phases are 0.1598×10^{-13} and 0.17468×10^{-3} kg, which correspond to drop diameters of 3.125 and 8063 μm, and ice particle diameters of 3.23754 and 8540 μm, respectively. Aerosols are divided into 67 bins with the minimum radius of 0.0041 μm. The domain in the model is 12 km in the vertical and 6 km in the radial direction. The grid size is 150 m and 300 m, respectively, in the radial and vertical direction. A time step of 2.5 s is used for condensation/evaporation of drops or deposition/sublimation of ice particles, 0.1 s for gas absorption, and 5 s for all other processes.

To simulate the evolution of trace gases in the air and in hydrometeors, the dynamic and microphysical equations are also applied to the mixing ratio of a gas species i in the air, $M_{a,i}$, and the mixing ratio in hydrometeors, $M_{h,i}$. These equations are given as

$$\frac{\partial M_{a,i}}{\partial t} = F_q\left(M_{a,i}\right) - D\left(M_{a,i}\right) + \left(\frac{\partial M_{a,i}}{\partial t}\right)_{\text{uptake}} + \left(\frac{\partial M_{a,i}}{\partial t}\right)_{\text{micro}} \quad (1)$$

ACPD
2, 875–903, 2002

and

$$\frac{\partial M_{h,i,k}}{\partial t} = F_q\left(M_{h,i,k}\right) - D\left(M_{h,i,k}\right) + \left(\frac{\partial M_{h,i,k}}{\partial t}\right)_{\text{uptake}} + \left(\frac{\partial M_{h,i,k}}{\partial t}\right)_{\text{micro}} \quad (2)$$

where the subscript k denotes the particle spectral bin number. The terms D and F_q represent the advective and turbulent transfer operators. The variation of these functions with location is implied. Also, the terms with subscripts 'uptake' and 'micro' represent mass transfer of chemical species between the gas phase and condensed phase due to uptake of gases by drops and ice particles, and that between different particle species due to microphysical processes.

2.2. Mass transfer between gas and hydrometeors

2.2.1. Gas interaction with droplets

The rate of mass transfer between gas phase and aqueous phase for chemical species i and a group of aqueous drops with radius of r and number concentration of N_r (per mole of air) is calculated using the following kinetic equation

$$\frac{dM_{d,i,r}}{dt} = \frac{3\eta D_{g,i} N_{Sh,i}}{RTr^2}\left(V_r N_r P_i - \frac{M_{d,i,r}}{H_i^*}\right), \quad (3)$$

where $M_{d,i,r}$ is the molar mixing ratio respect to air of gas species i inside drops with radius r, H^* is the effective Henry's law constant of species i, R is the universal gas constant, T is the temperature, $D_{g,i}$ is the diffusivity of gas species i in air, V_r is the volume of drops with radius r, P_i is the partial pressure of gas species i in the environment, $N_{Sh,i}$ is the mass ventilation coefficient (Sherwood number), and η is a factor to

ACPD
2, 875–903, 2002

account for the free-molecular effect on the mass transfer rate. This equation has the analytical solution

$$M_{d,i,\bar{r}_k}(\tau + \Delta\tau) = A(\tau) + [M_{d,i,\bar{r}_k}(\tau) - A(\tau)]\exp(B\Delta\tau), \quad (4)$$

where $\Delta\tau$ is the time step for gas dissolution, and

$$A(\tau) = \frac{4}{3}\pi\bar{r}_k^3 N_k P_i(\tau) H_i^*, \quad B = -\frac{3D_{g,i}N_{Sh,i}\eta}{\bar{r}_k^2 RTH_i^*}. \quad (5)$$

2.2.2. Freezing of droplets

The model treatment of gas interaction with ice hydrometeors is shown in Fig. 1. When droplets freeze, a fraction R_c of the gas is retained by the ice crystal and $(1 - R_c)$ released to the gas phase. The partitioning of the gas between the gas and ice phase is assumed to be instantaneous. The gas sequestered by the ice crystal is assumed to be fully retained; that is, no equilibrium is set up between the concentration of gas in the crystal and the gas phase. This is a valid assumption due to the slow diffusion of the gas through the crystal.

In this study, we perform five modeling simulations, each for the continental and maritime cloud, with R_c ranging from 0.0 to 1.0. The extreme case with retention coefficient equal to 0.0 means that the dissolved gas is transferred completely to the gas phase when a hydrometeor freezes. In the other extreme case of $R_c = 1$, the dissolved gas mass is retained fully by the resultant ice hydrometeor.

2.2.3. Growth of ice crystals by vapour diffusion

Growth of ice particles by diffusion of water vapour is assumed in the model to lead to burial of the trace gas molecules. Any molecules of gas that become attached to the surface of the growing ice crystal rapidly become buried by several monolayers of ice before they have a chance to desorb. As a sensitivity test we vary the fraction of

ACPD
2, 875–903, 2002

molecules that become permanently buried in terms of a "burial efficiency", β. A value of $\beta = 1$ assumes that all trace gas molecules that diffuse to the growing crystal surface become buried, while a lower value of β implies that a fraction β of the gas molecules that strike the crystal become buried and a fraction $(1 - \beta)$ remain in the gas phase. Gases with $\beta < 1$ are likely to be those with a weak interaction with the ice surface so can desorb at a rate comparable to the deposition rate of water molecules. The value of β will be related in some way to the mass accommodation coefficient of the gas and the adsorption enthalpy on a non-growing ice surface. In this study, we vary β between 0 and 1 as a sensitivity test.

2.2.4. Riming

Riming causes ice crystals to grow by accretion and freezing of supercooled water droplets. When riming occurs, the fraction R_c of the chemical species in the accreting droplet is retained in the rimed ice particle and a fraction $(1 - R_c)$ is released to the gas phase.

2.2.5. Sublimation and melting

When ice hydrometeors sublime we assume that the buried trace gas is released to the gas phase at a rate proportional to the mass of water evaporated. The gas is assumed to be uniformly distributed through the particle, thus we do not retain information on the radial distribution of the buried gas.

Upon melting, the buried gas mass is retained in the new droplet and used to calculate a liquid phase concentration. Gas-liquid mass transfer is then calculated as for other droplets.

ACPD
2, 875–903, 2002

3. Initial conditions and numerical experiments

3.1. Initial conditions

Numerical experiments were performed for continental and maritime conditions. For both cases an artificial thermodynamic profile representative of typical conditions was used. The profile produces a cloud with a base at 8–10°C (1.5–1.8 km) and a top at −25°C (7.0 km). For initialization, a warm bubble that produced a 2°C perturbation was applied for one time step at $t = 0$ in a region with radial distance of 450 m, at a height of 600 m.

The number concentration of aerosols large enough to act as cloud condensation nuclei (CCN) distinguishes the maritime and continental clouds. The CCN are assumed to be composed of ammonium sulfate, regardless of size, and the CCN concentrations are assumed to decrease exponentially with altitude with a scale height of 2.5 km (according to Pruppacher and Klett, 1997). The initial profiles of temperature, dew point temperature, and CCN spectra are shown in Fig. 2.

Because the main purpose of these simulations is to estimate to what extent the gases from the boundary layer can be transported to the free atmosphere and upper troposphere, the initial trace gas mixing ratio was arbitrarily assumed to be 1 ppbv and to be homogeneously distributed in the boundary layer, with a height of 1.5 km.

3.2. Numerical experiments

Numerical experiments were conducted to test the sensitivity of gas transport to the value of retention coefficient (R_c = 0, 0.25, 0.5, 0.75, and 1.0) and gas burial efficiency in growing ice crystals (β = 0, 0.01, 0.1, and 1.0). The experiments were repeated for the maritime and continental cloud types for a range of gas solubilities (effective Henry's law constant H^* between 0 and 10^9 mol dm^{-3} atm^{-1}). The simulations are listed in Table 1. Because we did not include concurrent gas phase chemical reactions in our model, all changes to the gas phase chemical species are induced by dynamical

ACPD
2, 875–903, 2002

transport, dissolution, adsorption, or exclusion of chemical species due to freezing of drops.

4. Results

4.1. Evolution of the cloud structure and precipitation

Figure 3 shows the time evolution of the cloud physical propertes (maximum values of water content, number concentrations of the different hydrometeors, vertical velocity, and rainfall rate). Figs. 4 and 5 show the spatial distributions of wind field, water content and number concentration of each hydrometeor for the continental and maritime clouds. In each case, the clouds begin to form after 8 min of simulation, and reach their peak updrafts 12 min later. While the maximum liquid water content (LWC), which mainly depends on the initial thermodynamic conditions, is similar in these two cases, the number concentration of drops as well as the properties of ice phase particles are quite different. The higher droplet concentration in the continental case leads to stronger competition for available water vapor for drop growth via diffusion and therefore restricts the growth of cloud droplets. As a consequence, drop growth by the collision-coalescence process is less efficient in the continental case. In contrast, the droplets in the maritime cloud reach sizes required for efficient collision-coalescence comparably faster than those in the continental case. One of the consequences of the low number concentration of large drops in the maritime case is that most of the drops were converted into graupel particles upon freezing, instead of ice crystals, as in the continental case. In addition, the rapid rise in supersaturation in the maritime cloud leads to faster production of ice crystals by vapor deposition. This is seen from Figs. 3d, e, and f, and Fig. 5.

The different liquid- and ice-phase microphysical processes in the two clouds are responsible for the reduced production of precipitation particles in the continental cloud compared with the maritime one (see Fig. 3h). Rain initiation and maximum rainfall

ACPD
2, 875–903, 2002

rate are also 5–7 min later in the continental case than in the maritime case. The maximum accumulated rain in the maritime cloud is 16 mm and is only 2.2 mm in the continental case. In both cases rain ended after around 64 min of simulation (here defined as rainfall rate less than 0.1 mm per hour). Such differences in the development of hydrometeors and precipitation have an important influence on the efficiency of gas transport to the upper troposphere as well as that of removal by wet deposition (wet deposition is calculated according to the fall velocities of the parent hydrometeors). This will be discussed in following sections.

4.2. The effect of retention coefficient on gas redistribution

Figures 6 and 7 show how the total gas transport depends on the gas solubility (H^*) and retention coefficient (R_c). The results are presented as integrated gas masses over the entire cloud outflow region, which is all air above 4 km altitude (a gas molar mass of 50 g mol^{-1} is assumed, though absolute gas amounts are not as important as relative amounts). The results are shown for the maritime and continental clouds at 64 min, which is after rainfall has ceased. As an example of one particular point on these contour plots, Fig. 8 shows the time evolution of gas abundance in different hydrometeors for $H^* = 10^7$ mol dm^{-3} atm^{-1} and $R_c = 1$. In the following discussion we examine the effect of changes in R_c and H^* on gas transport in the maritime case and then compare the maritime and continental cases.

Gas solubility in liquid hydrometeors and gas retention upon freezing both lead to a decrease in total gas mass in the outflow region. However, the effect of changes in one of these quantities depends on the value chosen for the other. For $R_c = 0$, changes in gas solubility (H^*) have very little effect on gas transport (Fig. 6). In this case, the transport of even highly soluble gases is similar to that of insoluble gases because gas expulsion from ice hydrometeors means that in large parts of the cloud the gas is present largely in the gas phase. The sensitivity of gas transport to H^* increases as R_c increases. For 100% gas retention upon freezing ($R_c = 1$), the gas mass in the outflow region is a factor 12 lower for a highly soluble gas than for an insoluble gas in

ACPD
2, 875–903, 2002

the maritime cloud.

Changes in R_c have little effect on the transport of low and moderately soluble gases but have a significant effect on the transport of highly soluble gases. For example, for $H^* = 10^4$ mol dm^{-3} atm^{-1} increasing R_c from 0 to 1 leads to only a 20% decrease in gas transport but for $H^* > 10^6$ gas transport decreases by a factor of 10. The effect of changes in R_c are approximately the same for all gas solubilities greater than 10^6 mol dm^{-3} atm^{-1} because this value of H^* represents complete partitioning into the liquid phase before ice formation.

The continental clouds (Fig. 7) show much less sensitivity to changes in R_c and H^* than the maritime clouds. For example, for highly soluble gases ($H^* > 10^6$ mol dm^{-3} atm^{-1}) a change in R_c from 0 to 1 leads to a factor 10 decrease in gas transport for the maritime cloud but only a factor 2 decrease for the continental cloud. Also, for $R_c = 1$, the decrease in gas transport for a highly soluble gas compared with an insoluble gas is a factor of 12 for the maritime cloud but only a factor of 2 for the continental cloud.

The much greater sensitivity of gas transport to gas solubility and retention for the maritime cloud compared with the continental cloud reflects differences in the microphysical processes, and in particular development of precipitation particles (Fig. 8). The main difference between the maritime and continental simulations is apparent in the trace gas abundance in the ice crystals and graupel particles: much more of the gas is present in graupel particles in the maritime case, which is consistent with the much higher graupel mass (see Sect. 4.1). The much more efficient precipitation processes occurring in the maritime cloud lead to efficient removal of the gas retained in large hydrometeors, and account for the large sensitivity of gas vertical transport to the choice of R_c and H^*. The higher efficiency of precipitation formation in the maritime cloud is also reflected in the amount of gas washed out (Table 2).

ACPD
2, 875–903, 2002

4.3. The effect of gas scavenging by ice particles on gas redistribution

Gas scavenging means the uptake and burial of trace gases by growing ice particles, and their release only upon ice particle evaporation or sublimation and is distinct from gas retention upon freezing, as discussed in the previous section.

Our simulations show that the efficiency of gas scavenging has little effect on gas transport except for relatively insoluble gases. For soluble gases, transport is dominated by uptake into droplets, for which gas retention upon freezing is then the determining factor. Insoluble gases, however, are present largely in the gas phase in the cloud core, so their transport might be expected to depend sensitively on the assumed uptake efficiency into growing ice crystals. However, even with highly efficient uptake into ice crystals (burial efficiency, $\beta = 1$) the effect on gas concentrations in the cloud outflow region is negligible. For example, for a moderately soluble gas with $H^* = 10^4$ mol dm^{-3} atm^{-1}, changing β from 0 to 1 reduces the gas abundance in the outflow region by only 30%.

Although the efficiency of gas uptake into growing crystals is not important for overall gas transport, it is important in determining the gas concentration in ice particles that may subsequently form cirrus clouds. Figure 9 shows the gas abundance in ice particles and graupel particles for cases C1 (with $\beta = 0$) and C7 (with $\beta = 1.0$). In each case $R_c = 1.0$. Ice particles dominate the hydrometeor population at the top of the cloud outflow region (see Figs. 4 and 5) and changing β from 0 to 1 increases the gas abundance in these ice particles by almost two orders of magnitude for the moderately soluble gas ($H^* = 10^4$ mol dm^{-3} atm^{-1}), although the changes calculated for the highly soluble gas (not shown) are negligible.

It is also worth noting that while gas uptake by ice increases the abundance of that tracer in the ice phase, the amount deposited by precipitation on the surface remains essentially unchanged due to the fact that the low solubility tracers are released to the gas phase once their ice-phase carriers fall below the 0°C level and begin to melt (see Table 2).

ACPD
2, 875–903, 2002

It should be stressed that these simulations represent upper and lower limits to the likely partitioning of gases into growing ice crystals. It is unlikely that any gases will become buried in growing ice crystals with 100% efficiency. However, moderately soluble gases (in this case $H^* = 10^4$ mol dm^{-3} atm^{-1}) are likely to become buried in growing crystals to some extent, and in such cases accurate knowledge of burial efficiencies will be important.

5. Discussion and summary

The Yin et al. (2001) model has been extended to include ice phase microphysics and trace gas transport. In representing these processes we have reduced the problem, for a given cloud evolution, to a three-dimensional parameter space of gas solubility, H^*, retention coefficient, R_c, and burial efficiency, β, acting to define the transport properties of a gas in a given cloud. The behaviour of the model as these parameters are varied has been explored for two idealised clouds — maritime and continental — and in each case, the variation of transport with H^*, R_c and β has been quantified.

The results show that the magnitude of total gas amount transported to the upper troposphere is controlled by gas solubility and gas retention coefficient. Gas transport is most sensitive to the value of retention coefficient when the solubility is high and, conversely, is most sensitive to solubility for high retention coefficients. Knowledge of the gas retention coefficient is more important for maritime clouds than continental clouds, with a high retention coefficient leading to higher wet removal of soluble tracers, according to the rainfall rate in the cloud. In the extreme case with all the dissolved gas being released from liquid drops upon freezing ($R_c = 0$), even the highly soluble gases can be transported to the free atmosphere and upper troposphere. This is consistent with the results of Barth et al. (2001), although different thermodynamic conditions are used for intialization of the simulations.

We have found that the total gas transport is relatively insensitive to direct gas uptake by growing ice particles (the gas burial efficiency). However, the burial efficiency

ACPD
2, 875–903, 2002

strongly controls the concentration of trace gases inside anvil ice crystals, which subsequently form cirrus clouds.

The results obtained with this cloud model are now quite exhaustive, in that they represent of all the key transport processes. A number of other processes, notably reactive chemistry, are not yet described. It is important at this stage to test the model results against observational data.

Our results also indicate where gaps in our understanding of basic physical processes could impact our ability to predict gas transport in mixed-phase clouds. For example, defining the gas retention coefficient of a highly soluble gas ($H^* > 10^6$ mol dm^{-3} atm^{-1}) in the range 0.5–1.0 allows the gas transport to be defined only to within a factor of 4 for a maritime cloud. However, for a moderately soluble gas ($H^* \sim 10^4$ mol dm^{-3} atm^{-1}) the uncertainty in gas transport would be less than a factor of 2.

Acknowledgements. This work was funded by the U.K. Natural Environment Research Council as part of the Upper Troposphere – Lower Stratosphere (UTLS-Ozone) thematic programme under grant GST/02/2433, and European Commission Fifth Framework Program, EVK2-2001-00057.

References

Barth, M. C., Stuart, A. L., and Skamarock, W. C.: Numerical simulations of the July 10 Stratospheric-Tropospheric Experiment: Radiation, Aerosols, and Ozone/Deep Convection storm: Redistribution of soluble tracers, J. Geophys. Res., 106, 12 381–12 400, 2001. 876, 878

Chatfield, R. B., and Crutzen, P. J.: Sulfur dioxide in the remote oceanic air: Cloud transport of reactive precursors, J. Geophys. Res., 89, 7111–7132, 1984. 876

Clapsaddle, C. and Lamb, D.: Sorption behavior of SO_2 on ice at temperature between -30°C and -5°C, Geophys. Res. Lett., 16, 1173–1176, 1989. 877

Clegg, S. M. and Abbatt J. P. D.: Uptake of gas-phase SO_2 and H_2O_2 by ice surface: dependence on partial pressure, temperature, and surface acidity, J. Phys. Chem., 105, 6630–6636, 2001. 877

Conklin, M. H. and Bales, R. C.: SO_2 uptake on ice sphere: Liquid nature of the ice-air interface, J. Geophys. Res., 98, 16 844–16 851, 1993. 877
Conklin, M. H., Sommerfeld, R. A., Layrd, S. K., and Villinski, J. E.: Sulfur dioxide reactions on ice surface: implications for dry deposition to snow, J. Atmos. Environ., 27A, 159–166, 1993. 877
Crutzen, P. J. and Lawrence, M. G.: The impact of precipitation scavenging on the transport of trace gases: A 3-dimensional model sensitivity study, J. Atmos. Chem., 37, 81–112, 2000. 877
Dickerson, R. R., Huffman, G. J., Luke, W. T., et al.: Thunderstorms: An important mechanism in the transport of air pollutants, Science, 235, 460–465, 1987. 876
Diehl, K., Mitra, S. K., and Pruppacher, H. R.: A laboratory study of the uptake of HNO_3 and HCl vapor by snow crystals and ice spheres at temperature between 0 and −40°C, J. Atmos. Environ., 29A, 975–981, 1995. 877
Diehl, K., Mitra, S. K., and Pruppacher, H. R.: A laboratory study on the uptake of HCl, HNO_3, and SO_2 gas by ice crystals and the effect of these gases on the evaporation rate of the crystals, Atmos. Res., 47/48, 235–244, 1998. 877
Hudson, P. K., Foster, K. L., Tolbert, M. A., et al.: HBr uptake on ice: Uptake coefficient, H_2O/HBr hydrate formation, and H_2O desorption kinetics, J. Phys. Chem., 105, 694–702, 2001. 877
Iribarne, J. V. and Pyshnov, T.: The effect of freezing on the composition of supercooled droplets — I. Retention of HCl, HNO_3, and NH_3, J. Atmos. Environ., 24A, 383–387, 1990. 878
Iribarne, J. V., Pyshnov, T., and Naik, B.: The effect of freezing on the composition of supercooled droplets — II. Retention of SO_2, J. Atmos. Environ., 24A, 389–395, 1990. 878
Lamb, D. and Blumenstein, R.: Measurement of the entrapment of sulfur dioxide by rime ice, Atmos. Environ., 21, 1765–1772, 1987. 878
Mari, C., Jacob, D. J., and Bechtold P.: Transport and scavenging of soluble gases in a deep convective cloud, J. Geophys. Res., 105, 22 255–22 267, 2000. 878
Mitra, S. K., Barth, S., and Pruppacher, H. R.: A laboratory study on the scavenging of SO_2 by snow crystals, Atmos. Environ., 24A, 2307–2312, 1990. 877
Prather, M. J. and Jacob, D. J.: A persistent imbalance in HO_x and NO_x photochemistry of the upper troposphere driven by deep tropical convection, Geophys. Res. Lett., 24, 3189–3192, 1997. 876
Pruppacher, H. R. and Klett, J. D.: Microphysics of Clouds and Precipitation, D. Reidel, pp. 714,

ACPD
2, 875–903, 2002

1997. 884
Reisin, T., Levin, Z., and Tzivion, S.: Rain production in convective clouds as simulated in an axisymmetric model with detailed microphysics. Part I: Description of the model, J. Atmos. Sci., 53, 497–519, 1996. 879, 880
Santachiara, G., Frodi, F., and Vivarelli, F.: Scavenging of SO_2 and HCl during growth of ice crystals by vapour diffusion, Atmos. Environ., 29, 983–987, 1995. 877, 878
Snider, J. R., Montague, D. C., and Vali, G.: hydrogen peroxide retention in rime ice, J. Geophys. Res., 97, 7569–7578, 1992. 878
Sommerfeld, R. A. and Lamb, D.: Preliminary measurements of SO_2 adsorbed on ice, Geophys. Res. Lett., 13, 349–351, 1986. 877
Tzivion, S., Feingold, G., and Levin, Z.: A efficient numerical solution to the stochastic collection equation, J. Atmos. Sci., 44, 3139–3149, 1987. 880
Valdez, M. P., Dawson, G. A., and Bales, R. C.: Sulfur dioxide incorporation into ice depositing from the vapor, J. Geophys. Res., 94, 1095–1103, 1989. 877
Yin, Y., Levin, Z., Reisin, T. G., and Tzivion, S.: The effects of giant cloud condensation nuclei on the development of precipitation in convective clouds — A numerical study, Atmos. Res., 53, 91–116, 2000. 879
Yin, Y., Parker, D. J., and Carslaw, K. S.: Simulation of trace gas redistribution by convective clouds – Liquid phase processes, Atmos. Chem. Phys., 1, 19–36, 2001. 876, 879, 889
Zondlo, M. A., Barone, S. B., and Tolbert, M. A.: Uptake of HNO_3 on ice under upper tropospheric conditions, Geophys. Res. Lett., 24, 1391–1394, 1997. 877

ACPD
2, 875–903, 2002

Table 1. List of numerical experiments conducted for the continental (C1–C9) and maritime (M1–M9) cases. The burial coefficient, β, is the fraction of gas molecular collisions on a growing ice crystal that results in uptake. The retention coefficient, R_c, is the fraction of gas retained by a hydrometeor upon freezing. See Sect. 3.2 for more details

Runs	Burial Coefficient (β)	Retention Coefficient (R_c)
C1, M1	0	1.0
C2, M2	0	0.75
C3, M3	0	0.5
C4, M4	0	0.25
C5, M5	0	0.0
C6, M6	0.01	1.0
C7, M7	0.1	1.0
C8, M8	1.0	1.0
C9, M9	0.1	0.0

ACPD
2, 875–903, 2002

Table 2. Integrated trace gas mass (kg) removed by wet deposition in the continental (C1–C9) and maritime (M1–M9) clouds. Only results for gases with effective Henry's law constants of 0, 10^4, and 10^7 mol dm^{-3} atm^{-1}, representative of insoluble, moderately soluble, and highly soluble gases, respectively, are shown here. Detailed definitions of these cases are given in Table 1

Runs	$H^* = 0$	10^4	10^7	Runs	$H^* = 0$	10^4	10^7
C1	0.0	0.69	1.81	M1	0.0	3.30	10.22
C2	0.0	0.66	1.67	M2	0.0	2.88	9.32
C3	0.0	0.63	1.55	M3	0.0	2.57	8.30
C4	0.0	0.61	1.43	M4	0.0	2.31	7.05
C5	0.0	0.59	1.31	M5	0.0	2.11	5.48
C6	0.02	0.79	1.83	M6	0.33	4.06	10.14
C7	0.02	0.79	1.85	M7	0.33	4.05	10.36
C8	0.02	0.79	1.86	M8	0.33	4.05	10.44
C9	0.02	0.68	1.36	M9	0.26	2.83	5.80

ACPD
2, 875–903, 2002

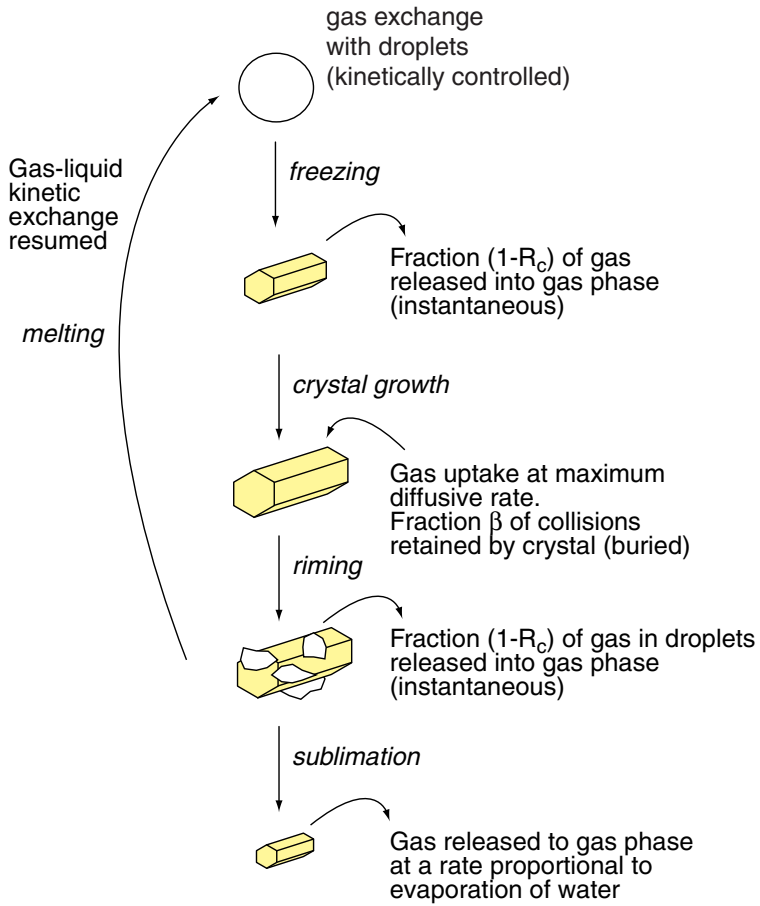

Fig. 1. Schematic of gas interaction with different hydrometeors used in this study.

ACPD

2, 875–903, 2002

Trace gas transport in mixed-phase convective clouds

Yin et al.

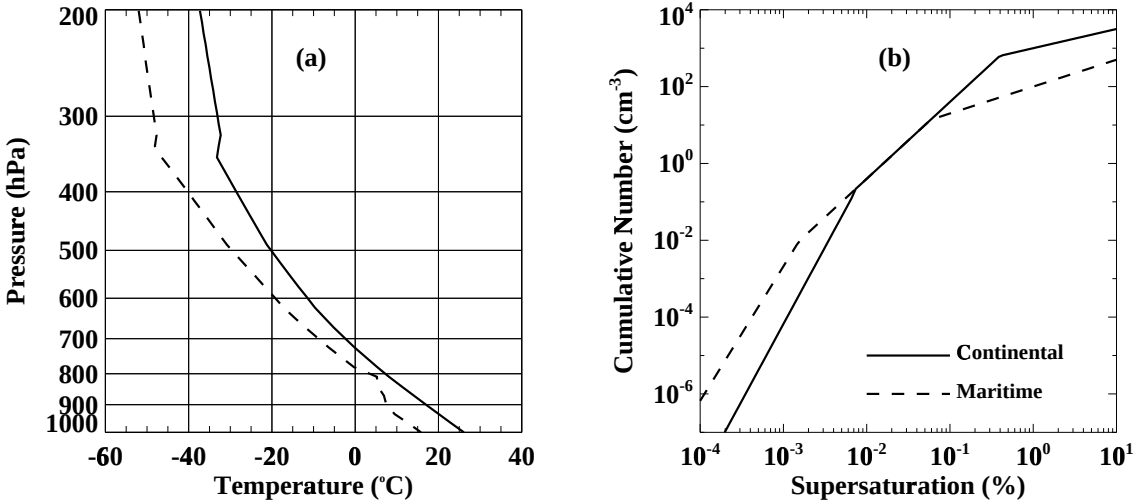

Fig. 2. **(a)** Initial profiles of temperature (solid line) and dew point temperature (dashed line), and **(b)** CCN spectra used in the present work.

ACPD

2, 875–903, 2002

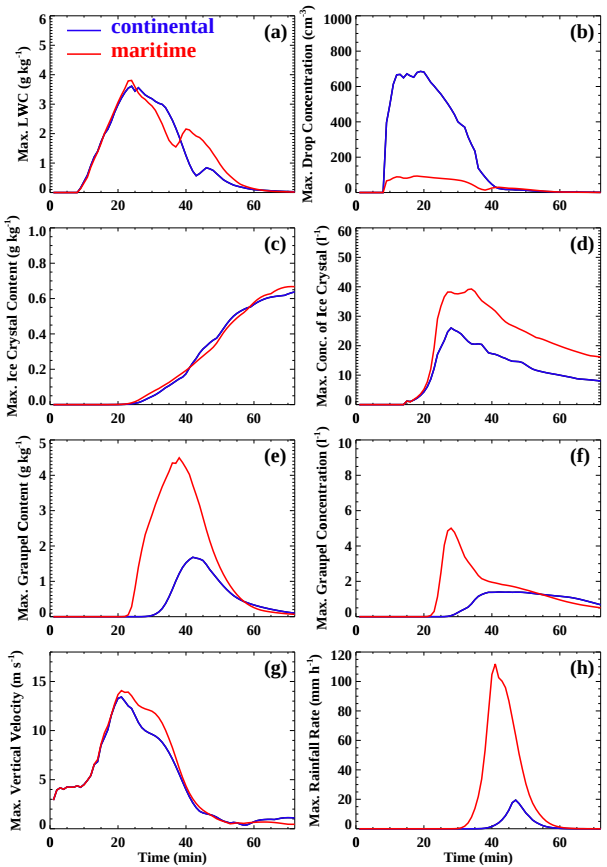

Fig. 3. Time-evolution of the maximum values of **(a)** liquid water content (LWC), **(b)** number concentration of drops, **(c)** water content of ice crystals, **(d)** number concentration of ice crystals, **(e)** water content of graupel particles, **(f)** number concentration of graupel particles, **(g)** vertical velocity, and **(h)** rainfall rate in the continental (blue curves), and maritime (red curves) cases.

ACPD
2, 875–903, 2002

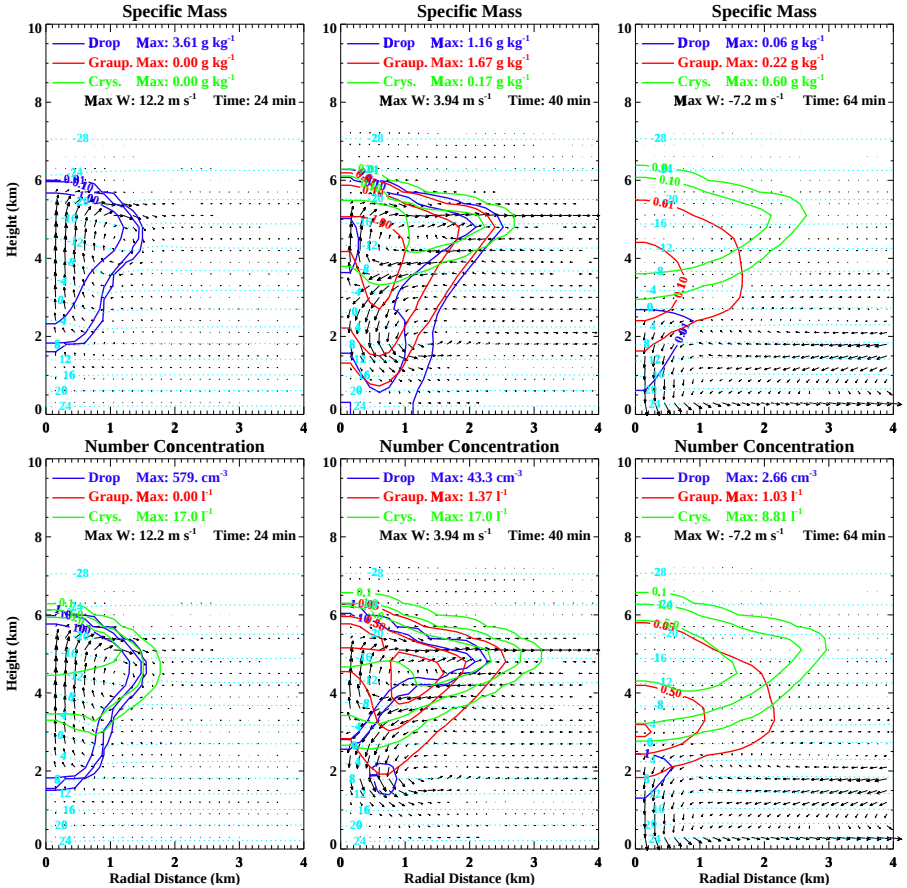

Fig. 4. Spatial distributions of specific mass (top panels) and number concentration (bottom panels) for drops, graupel and ice crystals at 24 min, 40 min, and 64 min of the continental simulation. 24 min is the time with peak cloud water content and 40 min is the time with peak graupel content. 64 min is the cloud dissipation stage. The horizontal dotted lines are isotherms and arrows are wind vectors.

ACPD
2, 875–903, 2002

Trace gas transport in mixed-phase convective clouds

Yin et al.

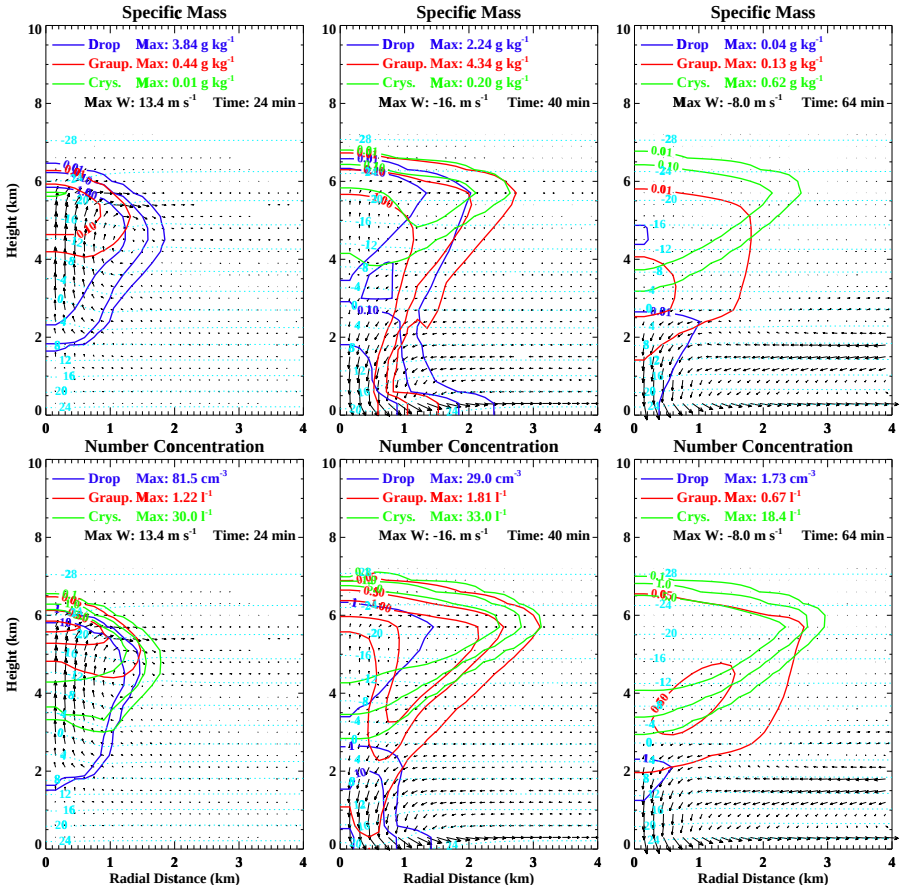

Fig. 5. Spatial distributions of specific mass (top panels) and number concentration (bottom panels) for drops, graupel and ice crystals at 24 min, 40 min, and 64 min of the maritime simulation. 24 min is the time with peak cloud water content and 40 min is the time with peak graupel content. 64 min is the cloud dissipation stage. The horizontal dotted lines are isotherms and arrows are wind vectors.

ACPD
2, 875–903, 2002

Trace gas transport in mixed-phase convective clouds

Yin et al.

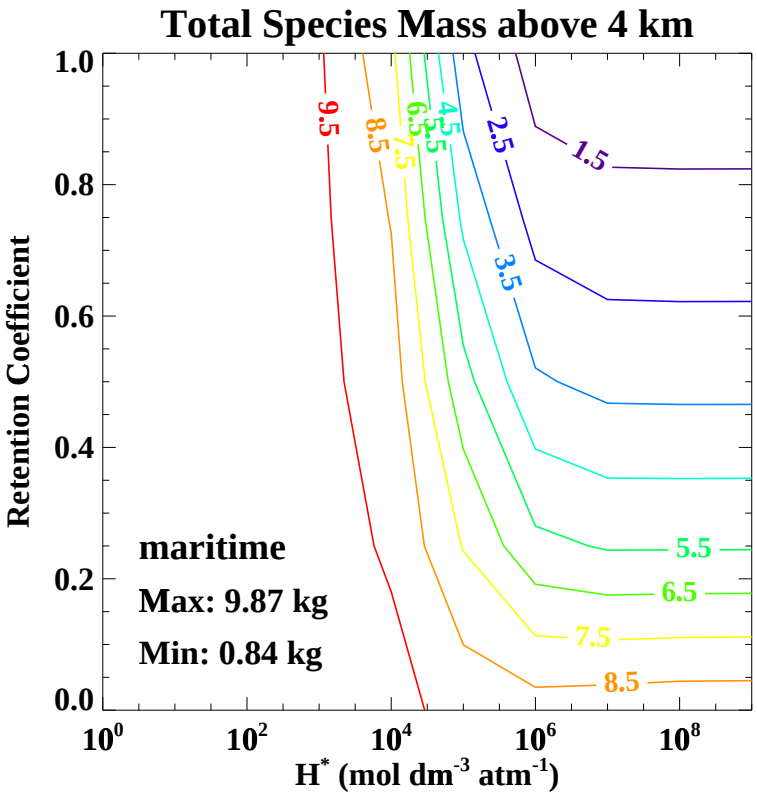

Fig. 6. Spatial integrated trace gas masses above 4 km (the main cloud outflow region) as a function of gas solubility and retention coefficient after 64 min of simulation of the maritime cloud. The gas burial coefficient β = 0.

ACPD
2, 875–903, 2002

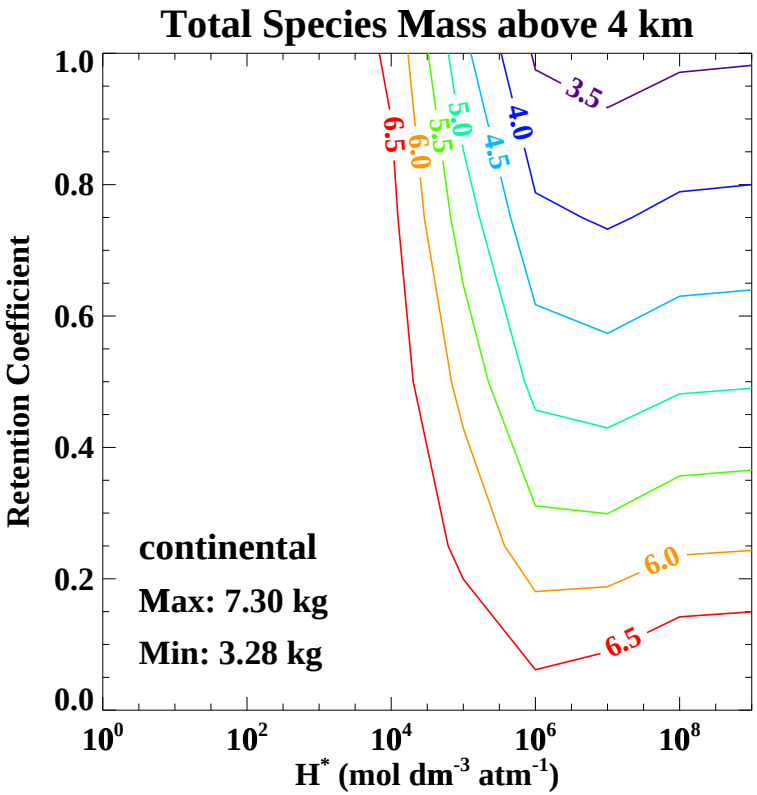

Fig. 7. Spatial integrated trace gas masses above 4 km (the main cloud outflow region) as a function of gas solubility and retention coefficient after 64 min of simulation of the continental cloud. The gas burial coefficient β = 0.

ACPD
2, 875–903, 2002

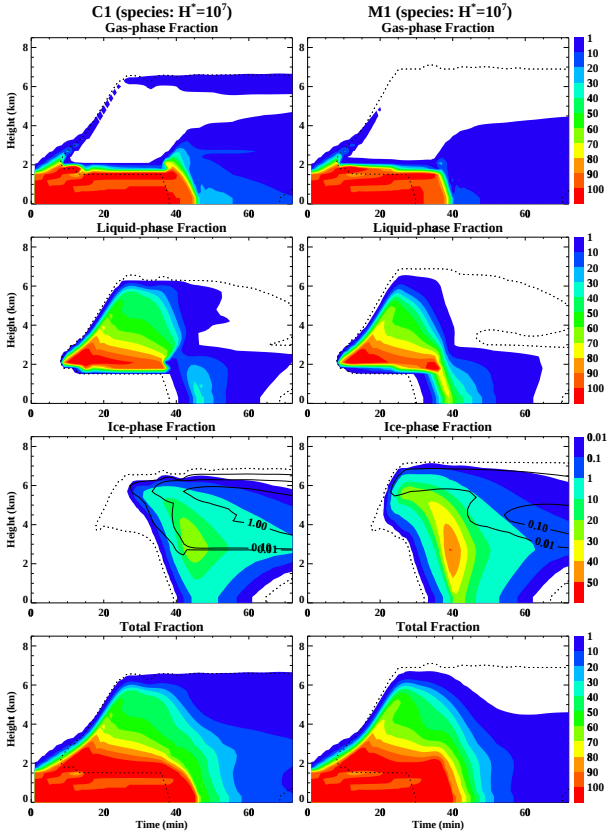

Fig. 8. Time-evolution of a soluble tracer ($H^* = 10^7$ mol dm^{-3} atm^{-1}) in the main updraft core of the continental cloud (left column) and maritime cloud (right column) with gas burial coefficient $\beta = 0$ and retention coefficient $R_c = 1$ (cases C1 and M1). The species abundance is expressed as a fraction of the initial boundary layer mixing ratio. The tracer abundance in ice crystals (black solid contours) is over-plotted on that in graupel (filled colour contours). The black dotted lines are isolines of 10^{-3} g kg^{-1} condensed water for liquid-phase, ice-phase, and total water content.

ACPD
2, 875–903, 2002

Trace gas transport in mixed-phase convective clouds

Yin et al.

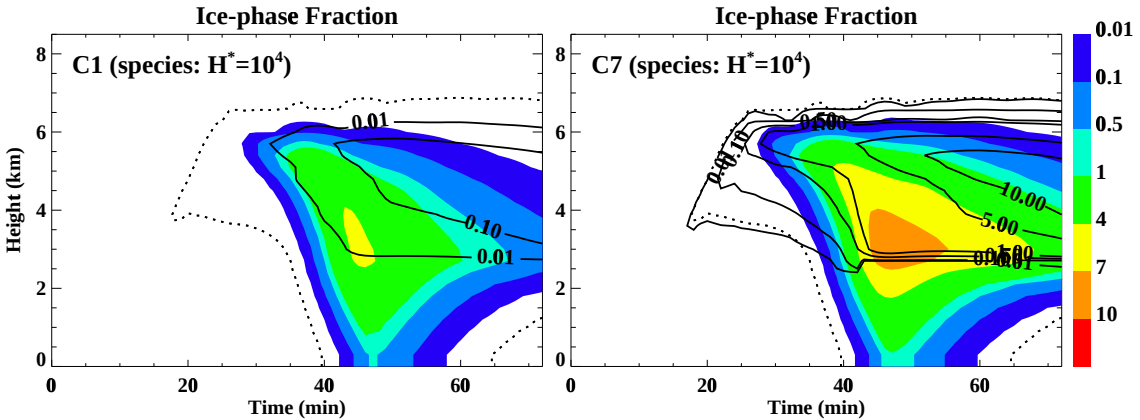

Fig. 9. The effect of gas burial in growing ice crystals on the abundance of a trace gas in ice crystals and graupel in a continental cloud. Results are shown as the time-evolution of a moderately soluble tracer (H^* = 10^4 mol dm^{-3} atm^{-1}) in the main updraft core for gas burial coefficient β = 0 (case C1, left column) and β = 1 (case C7, right column). The species abundance is expressed as a fraction of the initial boundary layer mixing ratio. The tracer abundance in ice crystals (black solid lines) is over-plotted on that in graupel (filled colour contours). The black dotted line is the isoline of ice-phase water content = 10^{-3} g kg^{-1}.

ACPD
2, 875–903, 2002